

# LLaVA-MLB: Mitigating and Leveraging Attention Bias for Training-Free Video LLMs

Leqi Shen<sup>1,2§\*</sup> Tao He<sup>4,5\*</sup> Guoqiang Gong<sup>3†</sup> Fan Yang<sup>1,2</sup> Yifeng Zhang<sup>3</sup>  
Pengzhang Liu<sup>3</sup> Sicheng Zhao<sup>2‡</sup> Guiguang Ding<sup>1,2‡</sup>

<sup>1</sup> School of Software, Tsinghua University <sup>2</sup> BNRist, Tsinghua University  
<sup>3</sup> JD.com <sup>4</sup> GRG Banking Equipment Co., Ltd. <sup>5</sup> South China University of Technology

## Abstract

Training-free video large language models (LLMs) leverage pretrained Image LLMs to process video content without the need for further training. A key challenge in such approaches is the difficulty of retaining essential visual and temporal information, constrained by the token limits in Image LLMs. To address this, we propose a two-stage method for selecting query-relevant tokens based on the LLM attention scores: compressing the video sequence and then expanding the sequence. However, during the compression stage, Image LLMs often exhibit a positional attention bias in video sequences, where attention is overly concentrated on later frames, causing early-frame information to be underutilized. To alleviate this attention bias during sequence compression, we propose Gridded Attention Pooling for preserving spatiotemporal structure. Additionally, we introduce Visual Summarization Tail to effectively utilize this bias, facilitating overall video understanding during sequence expansion. In this way, our method effectively **Mitigates and Leverages attention Bias (LLaVA-MLB)**, enabling the frozen Image LLM for detailed video understanding. Experiments on several benchmarks demonstrate that our approach outperforms state-of-the-art methods, achieving superior performance in both efficiency and accuracy. Our code will be released.

## 1 Introduction

The Video LLMs leverage large language models (Achiam et al., 2023; Chiang et al., 2023; Taori et al., 2023; Touvron et al., 2023a,b) (LLMs) for video-language reasoning, which can interpret video content and natural language instructions to generate contextually appropriate responses. Generally, Video LLMs can be categorized into

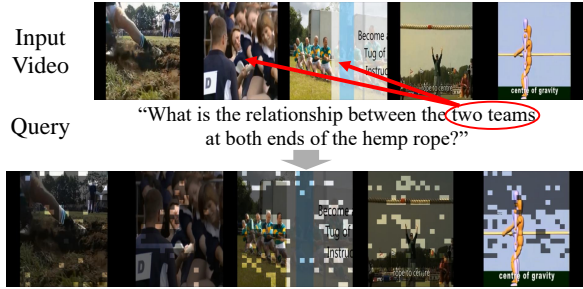


Figure 1: An example from ANet-QA (Yu et al., 2019) illustrates the positional attention bias. Out of the 2880 tokens from 5 sampled frames ( $5 \times 24 \times 24$ ), the 720 tokens with the highest attention scores are mostly concentrated in the last frame.

two main types: training-based and training-free. Training-based methods are fine-tuned on large-scale video datasets, allowing the models to adapt to the temporal nature of video content. However, these methods typically require the collection and annotation of extensive supervised fine-tuning datasets, along with substantial computational resources for training. In contrast, training-free methods directly leverage pretrained Image LLMs to interpret video content, without additional training. These methods improve the generalization performance of Image LLMs when applied to video data.

In these training-free methods, tokens from all video frames are fed together into the LLM. Due to the LLM token limits, Image LLMs struggle to process a large number of tokens per frame and maintain a long temporal context. To address this, we aim to input only the tokens that are relevant to the query. Specifically, we propose a two-stage framework: sequence compression and sequence expansion. First, we use the attention scores from the LLM to select query-relevant tokens within a video segment. Second, to further enhance the temporal context, we merge multiple compressed segments in the temporal dimension. These compressed tokens are then fed into the LLM to generate the final

<sup>§</sup>Work done during an internship at JD.com.

<sup>\*</sup>Equal contribution.

<sup>†</sup>Project leader. <sup>‡</sup>Corresponding authors.

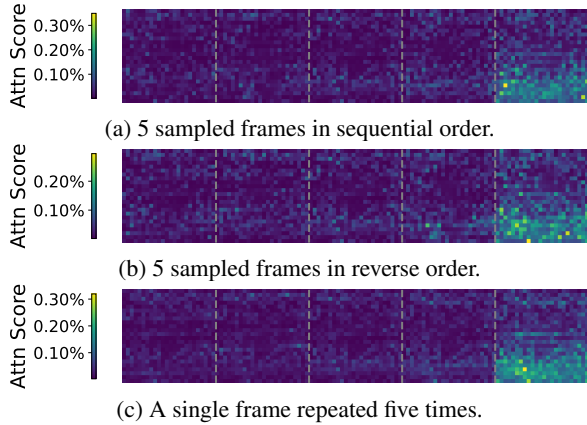


Figure 2: The average attention scores on ANet-QA. For each video, tokens from 5 sampled frames ( $5 \times 24 \times 24$ ) are input into the LLM. The attention score is computed using the last query token at 3<sup>th</sup> layer. Brighter areas correspond to higher attention values. (a) shows five sequential frames, and (b) shows them in reverse. In (c), a single frame is sampled and repeated five times.

output. This would enable more fine-grained and accurate token compression, thereby effectively expanding the spatiotemporal dimensions.

However, when compressing the sequence, we have found that a positional attention bias is evident at the tail of video sequences in Image LLMs. As shown in Figure 1, the example video showcases a complex multi-scene tug-of-war event. Although the query relates to earlier “two teams” scenes, the Image LLM incorrectly focuses high attention on the last, irrelevant frame. Additionally, Figure 2a quantifies the attention scores across the entire ANet-QA. We observe that most of the high attention tokens in the video are concentrated in the last frame, which is closer to the query. Out of the 2880 tokens from five sampled frames, we select the top 720 tokens. The average number of tokens retained in the last frame is 358.4, accounting for **49.8%** of the total selected tokens. Furthermore, similar attention biases are observed in Figure 2b and 2c, confirming that such a bias is consistent across different sequence compositions. This suggests that positional attention bias at the end of video sequences is inherent in Image LLMs, independent of the input’s semantic content.

Such attention bias negatively affects query-relevant token selection during sequence compression. If we retain video tokens with high attention scores in this manner, it becomes difficult to preserve information that is farther from the query. Potentially useful information from earlier frames may be discarded and not utilized by the model,

limiting the overall effectiveness.

To mitigate the attention bias inherent in video sequences for Image LLMs, we tackle the problem from two distinct angles, effectively **Mitigating and Leveraging attention Bias (LLaVA-MLB)**. First, we minimize the negative impact of attention bias during sequence compression. Second, we leverage the properties of attention bias for sequence expansion.

Specifically, on the one hand, to mitigate the concentration of selected high attention tokens towards the tail, we introduce a *Gridded Attention Pooling* module. This approach selects the most relevant visual tokens to the query within multiple local grids, ensuring that the selected visual tokens are evenly distributed across multiple frames in the spatiotemporal dimension. This method not only avoids the bias issue but also preserves the spatiotemporal structure of the visual tokens. On the other hand, the phenomenon of attention scores concentrating on the tail can be further leveraged for better global video understanding. To this end, we propose a *Visual Summarization Tail* module, which uses a large kernel pooling operation to generate a small token set that represents global summary information. These tokens are placed at the end of the visual sequence, allowing the query to focus more on the global context.

We evaluate our LLaVA-MLB across several tasks, including text generation (Maaz et al., 2024), open-ended VideoQA (Yu et al., 2019; Li et al., 2016), and multiple-choice VideoQA (Xiao et al., 2021; Mangalam et al., 2023). Our method outperforms existing approaches across all benchmarks. Compared to the previous SOTA model, SF-LLaVA (Xu et al., 2024b), our LLaVA-MLB achieves **0.8%** higher accuracy on ANet-QA and **4.2%** higher accuracy on EgoSchema, while requiring only **57%** of the pre-filling time.

Our contributions are summarized as follows:

- We identify a positional attention bias phenomenon in Image LLM for video understanding, where the attention scores between the query and the video are more concentrated on the tail-end visual tokens.
- We propose the *Gridded Attention Pooling* module to mitigate the bias phenomenon for enhanced token compression, and the *Visual Summarization Tail* module to leverage this bias phenomenon for better capturing global video information.
- We validate the effectiveness of the proposed method on multiple video understanding bench-

marks, demonstrating superior performance that exceeds current state-of-the-art methods, in terms of both efficiency and effectiveness.

## 2 Related Work

**Video LLMs.** Building on advancements in LLMs (Achiam et al., 2023; Chiang et al., 2023; Taori et al., 2023; Touvron et al., 2023a,b; Ouyang et al., 2022) and Image LLMs (Team et al., 2023; Liu et al., 2024a,b; Li et al., 2023a; Alayrac et al., 2022; Li et al., 2024; Liu et al., 2024c; Dai et al., 2023), researchers explore Video LLMs (Zhang et al., 2023b; Cheng et al., 2024; Maaz et al., 2024; Lin et al., 2023; Song et al., 2024a,b; Li et al., 2023b; Ma et al., 2023; Xu et al., 2024a; Zhang et al., 2024) for diverse applications in video-language comprehension. Video-LLaMA (Zhang et al., 2023b) enables video comprehension by combining frozen encoders and frozen LLMs with a Video Q-former. Video-ChatGPT (Maaz et al., 2024) introduces a new video instruction dataset for adapting the image-based LLaVA model to video tasks. MovieChat (Song et al., 2024a) implements an effective memory management mechanism for long videos. Chat-UniVi (Jin et al., 2024) applies multiscale dynamic visual tokens to represent images or video tokens. PLLaVA (Xu et al., 2024a) introduces a post-training method, adapting pre-trained Image LLMs for dense video understanding. LLaVA-NeXT-Video (Zhang et al., 2024) further fine-tunes image-based LLaVA-Next on video data, with LLaVA-Next-Video-DPO (Zhang et al., 2024) adding direct preference optimization. Nevertheless, most video LLMs rely on extensive fine-tuning with large-scale video datasets, which incurs significant computational costs.

**Training-Free Video LLMs.** By directly applying pretrained Image LLMs without additional training, training-free Video LLMs (Kim et al., 2024; Wu, 2024; Han et al., 2024; Xu et al., 2024b; Wang et al., 2024b; Zhang et al., 2023a; Wang et al., 2024a) present a cost-efficient option for video understanding. These training-free methods can be categorized into two types: caption-based (Wang et al., 2024b; Zhang et al., 2023a; Wang et al., 2024a) and vision-based (Kim et al., 2024; Wu, 2024; Han et al., 2024; Xu et al., 2024b). Caption-based methods convert videos into a series of densely sampled frame captions, allowing LLMs to respond to text queries based on these captions. However, these methods are limited by the quality of the caption

generation process. In this paper, we focus on vision-based methods, which rely on pretrained LLMs to process sampled frames directly for query response. FreeVA (Wu, 2024) explores different temporal pooling aggregation strategies on video features. SF-LLaVA (Xu et al., 2024b) employs a two-stream architecture to aggregate video features through pooling. Although these query-agnostic pooling methods reduce the token count per frame, allowing for longer temporal context, they significantly reduce spatial detail. To mitigate this, we aim to compress tokens by selecting those most relevant to the query.

Recent Free Video-LLM (Han et al., 2024) is also a query-conditioned method that uses query prompt information to guide the selection of regions of interest in the video. Our LLaVA-MLB differs significantly from Free Video-LLM. First, Free Video-LLM computes relevance scores using the global text features extracted from the CLIP text encoder, raising concerns about the granularity and accuracy of its computations. In contrast, our LLaVA-MLB employs attention scores generated by advanced LLMs. Second, rather than focusing on query-relevant regions, LLaVA-MLB focuses on query-relevant token-level information, achieving a more granular focus on critical video details.

**Token Compression for Vision LLMs.** Token compression has emerged as a crucial technique for improving the efficiency of vision LLMs. MobileVLM (Chu et al., 2023) designs an efficient projector between visual and text features, reducing the inference budget. LLaVA-Prumerge (Shang et al., 2024) exploits the sparsity observed in the visual encoder to dynamically select the most crucial visual tokens. FastV (Chen et al., 2024) proposes a versatile plug-and-play method for pruning visual tokens in LMM layers. LOOK-M (Wan et al., 2024) focus utilizes a text-prior technique to compress the KV cache.

However, these token compression are generally restricted by the limited frame length of input video sequences. To address this limitation, we propose a two-stage solution, involving both sequence compression and expansion, that enables the effective processing of longer video sequences using frozen Image LLMs.

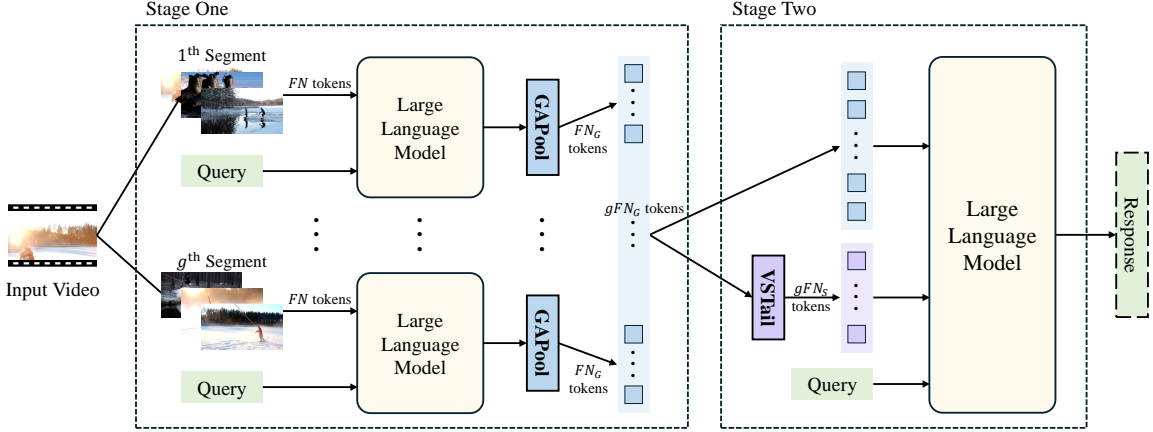


Figure 3: Illustration of LLaVA-MLB. We employ the two-stage SegAttn framework to extend the visual sequence. GAPool is introduced to mitigate attention bias, improving token compression. VSTail leverages attention bias to enhance overall video understanding.

### 3 Methodology

#### 3.1 Preliminary

The rapid advancements in Image LLMs stem from large-scale image-text datasets and image instruction data. However, extending this success to video requires extensive training on large video datasets, which is resource-intensive. Training-free Video LLMs provide an efficient alternative by leveraging pretrained Image LLMs without additional training.

Given a video, we first uniformly sample  $T$  frames. Each frame is independently processed by an image encoder, such as CLIP-L (Radford et al., 2021). The generated tokens are subsequently mapped into the language space through a pretrained projection layer. This process yields  $N = H \times W$  tokens per frame. These tokens from all sampled frames are concatenated to form the complete video input for the LLM, with a resolution of  $T \times H \times W$ . Finally, both the visual input  $\mathbf{V}$  and the textual query prompt  $\mathbf{Q}$  are input to the LLM to generate a response.

However, high token resolutions  $H \times W$  and large sampled frame length  $T$  may exceed the LLM’s maximum token limit. This challenge demands a careful trade-off between spatial detail and temporal span. Previous methods (Wu, 2024; Xu et al., 2024b; Han et al., 2024) attempt to reduce the token resolution using pooling, enabling longer frame sequences. However, the pooling operation significantly compromises spatial details. In contrast, we propose LLaVA-MLB, which employs query-relevant tokens to represent the input video, effectively preserving spatiotemporal detail with

fewer tokens.

#### 3.2 Segmented Attention Framework

In contrast to Free Video-LLM (Han et al., 2024), which relies on the CLIP text encoder to obtain query-relevant regions, our LLaVA-MLB selects query-relevant tokens with high attention scores from powerful LLMs. Traditional token pruning methods, however, only shorten the visual sequence, lacking the flexibility to expand it for temporal information. Therefore, we propose Segmented Attention Framework (SegAttn), a two-stage approach in Figure 3: sequence compression in the first stage and sequence expansion in the second stage. To simplify the process, we employ a strategy that compresses by a certain factor  $g$  and expands by the same amount.

Furthermore, as shown in Figure 2, a significant attention bias appears at the end of the video input, which distorts the selection of query-relevant tokens. To mitigate this bias, we propose Gridded Attention Pooling (GAPool) to preserve spatio-temporal structure. Alternatively, to leverage this bias, we propose Video Summarization Tail (VSTail) to enhance overall understanding.

Specifically, in stage one,  $T$  sampled frames are divided into  $g$  segments, with each segment containing  $F$  frames. For each segment, the  $F$  frames combined with the query prompt are input to the LLM to generate attention scores. Based on these scores, GAPool compresses  $FN$  tokens into  $FN_G$  tokens, where  $N_G = \frac{N}{g}$ .

In stage two, compressed tokens from all segments are aggregated, yielding a total of  $FN = gFN_G$  tokens. Moreover, VSTail appends  $gFN_S$

Method	# Input Tokens	Pre-filling Time		VCGBench	ANet-QA	EgoSchema
		Parallel	Sequential	Avg Score	Accuracy/Score	Accuracy
SF-LLaVA (Xu et al., 2024b)	3680	0.9659 s		3.04	55.5/3.4	47.2
LLaVA-MLB <sup>G</sup>	2880	<b>0.5473</b> s	<b>0.7352</b> s	3.06	<b>56.3/3.4</b>	<b>51.4</b>
LLaVA-MLB <sup>G+S</sup>	2880 + 240	0.5701 s	0.7579 s	<b>3.11</b>	55.6/3.3	<b>51.4</b>

Table 1: Efficiency comparisons using 7B LLMs. # Input Tokens denotes the number of tokens fed into the LLM for response generation. The pre-filling time is the time the model takes to generate the first output token. Parallel and Sequential refer to the compression of stage one conducted in parallel and sequentially, respectively. LLaVA-MLB<sup>G</sup> denotes SegAttn with GAPool. LLaVA-MLB<sup>G+S</sup> denotes SegAttn with both GAPool and VSTail, where VSTail introduces 240 additional summary tokens.

summary tokens at the end of the sequence, where  $N_S \ll N$ . The final response is generated from these tokens and the query prompt.

### 3.3 Gridded Attention Pooling

In stage one, we obtain attention scores from the pre-filling phase of the LLM. We leverage the attention scores from the shallow layers to identify tokens strongly associated with the query. Shallow layer scores are beneficial for two reasons: (1) According to (Chen et al., 2024; Wang et al., 2023), attention distribution is typically more balanced in shallow layers, where information is assembled to form semantic representations. Therefore, high attention scores in shallow layers help to capture query-relevant tokens. (2) Shallow layers are computationally efficient, as they avoid the need to propagate through the entire LLM. In particular, we utilize attention scores from the  $k^{\text{th}}$  layer’s last query token, where  $k = 3$ .

Due to attention bias, high attention scores often concentrate on tokens at the end of visual sequences. To mitigate this issue, we propose GAPool to select the most relevant visual tokens within multiple local grids, which maintains the sequence’s spatiotemporal structure. Specifically, GAPool divides  $FN$  tokens of each segment into grids:

$$\begin{aligned}
F \times N &= F \times H \times W \\
&= F \times (H_G G_h) \times (W_G G_w) \\
&= (F H_G W_G) \times G_h \times G_w \\
&= (F N_G) \times G_h \times G_w, \quad (1)
\end{aligned}$$

where  $G_h$  and  $G_w$  denote the grid height and weight.  $H_G$  and  $W_G$  denote the number of grids along the height and width.  $N_G$  is the total number of grids per frame. From each grid, GAPool selects the query-relevant token with the highest attention

score:

$$(p_*, q_*) = \arg \max_{1 \leq p \leq G_h, 1 \leq q \leq G_w} \mathbf{A}_{pq}^{G_{fij}} \quad (2)$$

where  $\mathbf{A}^{G_{fij}}$  denotes the attention scores of the grid located at the  $i^{\text{th}}$  row and  $j^{\text{th}}$  column in the  $f^{\text{th}}$  frame. In  $G_{fij}$ , we output only the token at position  $(p_*, q_*)$ . Therefore, we effectively compress the segment sequence into  $FN_G$  tokens, corresponding to a resolution of  $F \times H_G \times W_G$ , achieving a compression rate of  $g = G_h \times G_w$ .

To simplify the sequence expansion in stage two, the sequence expansion factor is set to match the compression factor of each segment sequence. We concatenate the compressed tokens from all segments, totaling  $FN = gF \frac{N}{g} = gFN_G$  tokens. Finally, these compressed tokens from  $T = gF$  sampled frames are combined with a query prompt to produce the final response in the LLM.

### 3.4 Video Summarization Tail

In contrast to GAPool, which mitigates attention bias in the selection of query-relevant tokens, VSTail leverages the concentration of attention at the visual input’s tail. VSTail implements a summary branch that applies large-kernel pooling to the stage one output, creating a small token set as the new tail for the visual input. This tail corresponds to regions with high attention scores, enhancing the overall understanding of the video.

Specifically, on the  $gF \times H_G \times W_G$  tokens from stage one, we apply average pooling with a large kernel size defined as  $S_h \times S_w$ . Each frame is downsampled from  $H_G \times W_G$  to  $H_S \times W_S$ , where  $H_S = \frac{H_G}{S_h}$ ,  $W_S = \frac{W_G}{S_w}$ . Consequently, the summary sequence has  $gFN_S = gF \times H_S \times W_S$  tokens, where  $N_S \ll N$ . Each token represents a receptive field of size  $P_h \times P_w = (G_h S_h) \times (G_w S_w)$  in the original input. The appended sequence at the visual input’s tail serves as a summary of the input video.

Method		LLM Size	Vision Encoder	VCGBench (Score)					
				CI	DO	CU	TU	CO	Avg
Training-based Video LLMs	Video-LLaMA (Zhang et al., 2023b)	7B	CLIP-G	1.96	2.18	2.16	1.82	1.79	1.98
	Video-LLaMA2 (Cheng et al., 2024)	7B	CLIP-L	3.16	3.08	3.69	2.56	3.14	3.13
	Video-ChatGPT (Maaz et al., 2024)	7B	CLIP-L	2.50	2.57	2.69	2.16	2.20	2.42
	MovieChat (Song et al., 2024a)	7B	CLIP-G	2.76	2.93	3.01	2.24	2.42	2.67
	VideoChat (Li et al., 2023b)	7B	CLIP-G	2.23	2.50	2.53	1.94	2.24	2.29
	Vista-LLaMA (Ma et al., 2023)	7B	CLIP-G	2.44	2.64	3.18	2.26	2.31	2.57
	LLaVA-NeXT-Video (Zhang et al., 2024)	7B	CLIP-L	3.39	3.29	3.92	2.60	3.12	3.26
	LLaVA-NeXT-Video-DPO (Zhang et al., 2024)	7B	CLIP-L	3.64	3.45	4.17	2.95	4.08	3.66
Training-free Video LLMs	IG-VLM (Kim et al., 2024)	7B	CLIP-L	3.11	2.78	3.51	2.44	3.29	3.03
	SF-LLaVA (Xu et al., 2024b)	7B	CLIP-L	3.09	2.70	3.57	<b>2.52</b>	3.35	3.04
	<b>LLaVA-MLB<sup>G</sup></b>	7B	CLIP-L	3.18	<b>2.85</b>	3.55	2.45	3.29	3.06
	<b>LLaVA-MLB<sup>G+S</sup></b>	7B	CLIP-L	<b>3.22</b>	2.83	<b>3.61</b>	<b>2.52</b>	<b>3.38</b>	<b>3.11</b>

Table 2: Results of text generation using 7B LLMs. The upper part shows methods trained on video data, while the lower part displays training-free Video LLMs. For the training-free method, the best metric is highlighted in bold.

Method		LLM Size	Vision Encoder	Open-Ended VideoQA		Multiple Choice VideoQA	
				ANet-QA Accuracy/Score	TGIF-QA Accuracy/Score	NExTQA Accuracy	EgoSchema Accuracy
Training-based Video LLMs	Video-LLaMA (Zhang et al., 2023b)	7B	CLIP-G	12.4/1.1	-	-	-
	Video-LLaMA2 (Cheng et al., 2024)	7B	CLIP-L	50.2/3.3	-	-	51.7
	Video-ChatGPT (Maaz et al., 2024)	7B	CLIP-L	35.2/2.7	51.4/3.0	-	-
	Video-LLaVA (Lin et al., 2023)	7B	ViT-L	45.3/3.3	70.0/4.0	-	-
	MovieChat (Song et al., 2024a)	7B	CLIP-G	45.7/3.4	-	-	-
	MovieChat+ (Song et al., 2024a)	7B	CLIP-G	48.1/3.4	-	54.8	-
	Video-Chat (Li et al., 2023b)	7B	CLIP-G	26.5/2.2	34.4/2.3	-	-
	Vista-LLaMA (Ma et al., 2023)	7B	CLIP-G	48.3/3.3	-	60.7	-
	PLLaVA (Xu et al., 2024a)	7B	CLIP-L	56.3/3.5	77.5/4.1	-	-
	LLaVA-NeXT-Video (Zhang et al., 2024)	7B	CLIP-L	53.5/3.2	-	-	-
LLaVA-NeXT-Video-DPO (Zhang et al., 2024)	7B	CLIP-L	60.2/3.5	-	-	-	
Training-free Video LLMs	FreeVA (Wu, 2024)	7B	CLIP-L	51.2/ <b>3.5</b>	-	-	-
	IG-VLM (Kim et al., 2024)	7B	CLIP-L	54.3/3.4	73.0/4.0	63.1	35.8
	Free Video-LLM (Han et al., 2024)	7B	CLIP-L	54.8/3.4	77.8/4.1	-	-
	SF-LLaVA (Xu et al., 2024b)	7B	CLIP-L	55.5/3.4	78.7/ <b>4.2</b>	64.2	47.2
	<b>LLaVA-MLB<sup>G</sup></b>	7B	CLIP-L	<b>56.3/3.4</b>	78.6/4.1	67.3	<b>51.4</b>
	<b>LLaVA-MLB<sup>G+S</sup></b>	7B	CLIP-L	55.6/3.3	<b>78.8/4.1</b>	<b>67.5</b>	<b>51.4</b>

Table 3: Results of open-ended VideoQA and multiple choice VideoQA using 7B LLMs.

### 3.5 Efficiency Analysis

In our framework, these hyper-parameters directly influence the model’s efficiency,  $F$ ,  $k$ ,  $g = G_h \times G_w$ , and  $S_h \times S_w$ .

$F$  denotes the number of frames per segment. In stage one, the attention score is computed from the  $k^{\text{th}}$  layer, enabling the LLM to stop forward propagation at this early layer, thereby saving significant computational time. In stage two, the sequence expansion factor is set equal to the compression factor  $g$  from stage one, where  $g$  is determined by the GAPool’s grid size  $G_h \times G_w$ . In VSTail, the pooling kernel size  $S_h \times S_w$  determines the number of generated summary tokens.

Furthermore, in stage one, we are able to apply parallel compression to multiple segments, effectively reducing inference time. When sufficient hardware resources are available, a parallel strat-

egy can be adopted. However, when only a single GPU is available, the sequential strategy remains efficient, as stage one only requires a shallow LLM, which does not result in significant time overhead.

In Table 1, we conduct an efficiency comparison between our method and the state-of-the-art SF-LLaVA (Xu et al., 2024b). Both SF-LLaVA and our method are built upon LLaVA-NeXT (Liu et al., 2024b). With just **57%** pre-filling time, LLaVA-MLB<sup>G</sup> surpasses SF-LLaVA by **0.8%** accuracy on ANet-QA and by **4.2%** on EgoSchema. Although implemented as a two-stage framework, our proposed LLaVA-MLB surpasses previous approaches in both performance and efficiency.

## 4 Experiments

We conduct evaluations across three tasks: text generation, open-ended VideoQA, and multiple choice

Segment Length $F$	# Tokens $gFN_G$	Pre-filling Time		ANet-QA Accuracy/Score
		Parallel	Sequential	
3	1728	0.3514 s	0.4788 s	55.0/3.3
4	2304	0.4519 s	0.6071 s	55.2/3.3
5*	2880	0.5473 s	0.7352 s	<b>56.3/3.4</b>
6	3456	0.6686 s	0.9018 s	<b>56.8/3.4</b>

Table 4: Ablation study on segment length  $F$  in LLaVA-MLB<sup>G</sup>. # tokens denotes the final visual input length, calculated as the sum of the compression tokens across all segments.

The $k^{\text{th}}$ Layer Attention Score	Pre-filling Time		ANet-QA Accuracy/Score
	Parallel	Sequential	
2	0.5459 s	0.7105 s	55.3/3.3
3*	0.5473 s	0.7352 s	<b>56.3/3.4</b>
5	0.5694 s	0.8040 s	55.8/3.4
8	0.5986 s	0.9064 s	56.0/3.4
10	0.6188 s	0.9735 s	55.9/3.4

Table 5: Ablation study on the  $k^{\text{th}}$  layer attention score in LLaVA-MLB<sup>G</sup>. We use attention score from the  $k^{\text{th}}$  layer for GAPool.

VideoQA. We introduce benchmarks and metrics for each task individually and implementation details in Appendix A.

#### 4.1 Comparisons with State-of-the-Arts

In Table 2, we report the performance of the text generation task evaluated on VCGBench using 7B LLMs. LLaVA-MLB<sup>G+S</sup> shows significant improvement over LLaVA-MLB<sup>G</sup> in CU, TU, and CO, confirming the effectiveness of VSTail, which appends a summary sequence to the visual input tail to enhance overall video understanding. Compared to prior state-of-the-art methods, our model achieves comparable performance in CU, TU, and CO. Notably, our model achieves significant improvements in both CI and DO. Compared to IG-VLM, LLaVA-MLB<sup>G+S</sup> improves the CI score by **0.11%**, and LLaVA-MLB<sup>G</sup> enhances the DO score by **0.07%**, highlighting our model’s superior ability to capture fine-grained details in video content.

Table 3 presents a comparison between our LLaVA-MLB and previous training-free methods on both open-ended VideoQA and multiple choice VideoQA tasks, utilizing 7B LLMs. For open-ended VideoQA, LLaVA-MLB<sup>G</sup> achieves comparable performance on TGIF-QA and increases accuracy by **0.8%** on ANet-QA. For multiple-choice VideoQA, LLaVA-MLB<sup>G+S</sup> demonstrates marked improvements, surpassing SF-LLaVA by **3.3%** accuracy on NEXtQA and **4.2%** accuracy on EgoSchema.

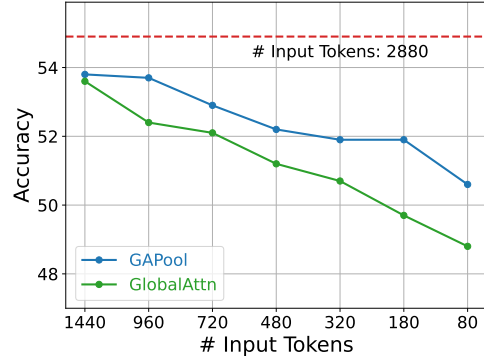


Figure 4: Ablation study on GAPool in LLaVA-MLB<sup>G</sup> using a 5-frame segment on ANet-QA. The red dashed line indicates the accuracy without compression. The number of the tokens fed into stage two is denoted by # input tokens. In GAPool, 1440, 960, 720, 480, 320, 180, and 80 indicate grid sizes of  $1 \times 2$ ,  $1 \times 3$ ,  $2 \times 2$ ,  $2 \times 3$ ,  $3 \times 3$ ,  $4 \times 4$ , and  $6 \times 6$ .

Grid Size $G_h \times G_w$	# Frames $g \times F$	Pre-filling Time		ANet-QA Accuracy/Score
		Parallel	Sequential	
$1 \times 2$	10	0.4419 s	0.5044 s	55.8/3.3
$2 \times 2^*$	20	0.5473 s	0.7352 s	<b>56.3/3.4</b>
$2 \times 3$	30	0.6940 s	1.0072 s	56.1/3.4
$2 \times 4$	40	0.7800 s	1.2175 s	54.6/3.3

Table 6: Ablation study on GAPool in LLaVA-MLB<sup>G</sup>. # Frames denotes the total sampled frames  $g \times F = (G_h G_w) \times F$ .

In Appendix B.1, we show the results with 34B LLMs, which confirm our model’s robustness and generalizability.

#### 4.2 Ablation Study on SegAttn Framework

**Effect of Segment Length  $F$ .** In Table 4, we evaluate our LLaVA-MLB<sup>G</sup> with various segment lengths. The frame number per segment  $F$  determines the total sampled frames  $gF$  from the input video. Increasing the sequence length provides more temporal information from the videos, leading to improved performance on ANet-QA as the frame length increases. Using  $gF = (G_h G_w)F = 4 \times 6 = 24$  sampled frames, we achieve a notable accuracy of **56.8%** on ANet-QA. However, a greater frame number implies more tokens for the LLM to process, which increases inference time. To balance efficiency and accuracy, we set  $F$  to 5. **Effect of the  $k^{\text{th}}$  Layer Attention Score.** Table 5 shows the effect of attention score from different layers in LLaVA-MLB<sup>G</sup>. As  $k$  grows, additional layers are required for the LLM inference in stage one, resulting in longer inference times. The third shallow layer obtains the best performance (**56.3%**

Pooling Size $S_h \times S_w$	Receptive Field $P_h \times P_w$	Frame Size $H_S \times W_S$	# Input Tokens $gFN_G + gFH_SW_S$	VCGBench Avg Score	ANet-QA Accuracy/Score	EgoSchema Accuracy
-	-	-	2880 + 0	3.06	<b>56.3/3.4</b>	51.4
12 × 12	24 × 24	1 × 1	2880 + 20	<b>3.12</b>	54.6/3.3	51.8
6 × 6	12 × 12	2 × 2	2880 + 80	<b>3.12</b>	55.1/3.3	51.4
4 × 4	8 × 8	3 × 3	2880 + 180	3.10	55.2/3.3	<b>52.0</b>
3 × 4*	6 × 8	4 × 3	2880 + 240	3.11	55.6/3.3	51.4
3 × 3	6 × 6	4 × 4	2880 + 320	3.09	55.0/3.3	50.8
2 × 3	4 × 6	6 × 4	2880 + 480	3.08	55.1/3.3	51.4
2 × 2	4 × 4	6 × 6	2880 + 720	3.06	55.8/3.4	51.0

Table 7: Ablation study on VSTail’s pooling size in LLaVA-MLB<sup>G+S</sup>. Receptive field is determined by the GAPool grid size and the VSTail pooling size,  $P_h \times P_w = (G_h S_h) \times (G_w S_w)$ . Frame size denotes the token size per frame in the VSTail summary sequence,  $H_S \times W_S = \frac{H}{P_h} \times \frac{W}{P_w}$ . # input tokens consists of  $gFN_G = gF \frac{N}{g}$  compressed tokens from stage one and  $gFH_SW_S$  tokens from VSTail.

Accuracy) with high efficiency, leading us to select  $k = 3$ .

### 4.3 Ablation Study on GAPool

**Effect of using a single segment.** In Figure 4, we conduct experiments in LLaVA-MLB<sup>G</sup> using a single 5-frame segment on ANet-QA. In the case of a single segment, we extract the compression tokens in stage one and input them directly into the LLM in stage two, without merging tokens from additional segments. In GlobalAttn, the tokens with the top- $\frac{2880}{G_h G_w}$  attention scores are selected as the final input into the LLM. Across various compression rates, GAPool consistently outperforms GlobalAttn by better selecting query-relevant tokens. Our grid-based token selection strategy preserves the spatiotemporal structure of video tokens, effectively mitigating attention bias during sequence compression.

**Effect of Grid Size  $G_h \times G_w$ .** Table 6 presents the impact of GAPool’s grid size  $G_h \times G_w$  in LLaVA-MLB<sup>G</sup>. In the two-stage SegAttn, the temporal dimension is expanded in alignment with the compression ratio  $g = G_h G_w$ . We find that when the sampled frame number surpasses 20, accuracy begins to degrade with increasing frames. This is likely due to the information loss incurred by higher compression ratios. A lower compression rate preserves detail, while a higher frame number introduces more temporal information, both of which need careful balancing. The optimal **56.3%** accuracy is achieved with a grid size of  $G_h \times G_w = 2 \times 2$ .

### 4.4 Ablation Study on VSTail

**Effect of Pooling Size  $S_h \times S_w$ .** Table 7 presents an ablation study on the pooling size  $S_h \times S_w$  in

VSTail for LLaVA-MLB<sup>G+S</sup>. A larger pooling size enlarges the receptive field of the summary token, leading to a smaller frame size in the summary sequence. As a result, each token in the sequence conveys a more comprehensive summary. Although VSTail shows limitations on ANet-QA, using one summary token per frame yields the highest average score of **3.12%** on VCGBench. As pooling size decreases, VCGBench performance also declines, potentially due to an attention bias toward the visual input’s tail. As depicted in Figure 2, the final  $\sim 300$  tokens exhibit a significantly higher attention score, suggesting that the optimal length of the summary sequence should ideally not exceed 300 tokens. Given VSTail’s performance on various datasets, we set  $S_h \times S_w = 3 \times 4$ , resulting in 240 summary tokens.

In Appendix B.2, we further analyze the impact of VSTail’s summary sequence position.

## 5 Conclusion

In this paper, we present a novel approach LLaVA-MLB for training-free video understanding in large language models, particularly focusing on mitigating attention bias in video sequences for Image LLMs. To mitigate the concentration of selected high attention tokens towards the tail, we propose Gridded Attention Pooling to preserve the spatiotemporal structure of video sequences. Alternatively, we propose Visual Summarization Tail to leverage this bias for better global video understanding. In this way, our LLaVA-MLB effectively selects query-relevant tokens, enabling detailed video comprehension in frozen Image LLMs. Extensive experiments validate the effectiveness of LLaVA-MLB on various video understanding

tasks. Our model surpasses current training-free approaches in both efficiency and accuracy.

## Limitations

**Query-relevant Token Selection.** Although GAPool effectively selects the most relevant token within each non-overlapping grid, it fails to capture all tokens associated to the query-relevant object. This limitation arises from the inherent attention bias in image LLMs, which causes the model to prioritize tokens at the end of the video sequence, hindering the selection of query-relevant object tokens. To mitigate this issue, our GAPool ensures that each grid contains a token with a high attention score, thereby preserving the spatiotemporal structure.

In addition, Free Video-LLM (Han et al., 2024) selects query-relevant regions by incorporating an additional text encoder, which introduces extra parameters. However, due to discrepancies between the text encoder and the image LLM, its performance is inferior (see Table 3).

**Lightweight Fine-tuning vs. Training-free Methods.** While lightweight fine-tuning from image LLMs to video can improve performance with minimal resources, it requires maintaining multiple specialized model checkpoints. In contrast, our LLaVA-MLB leverages a single pre-trained image LLM for both image and video understanding without modification. This makes our method particularly attractive for edge devices and real-time applications where efficiency is critical.

**Attention Bias.** As highlighted in Section 1, attention bias is an inherent challenge in image LLMs for video understanding. Since training-free video LLMs preserve the original image LLM weights, this bias remains unaltered in the final processing stage. Our LLaVA-MLB approach does not eliminate the bias but instead mitigates and leverages it to construct video input sequences with rich spatiotemporal information. To directly address this issue, fine-tuning could be a valuable direction for future research.

## References

Josh Achiam, Steven Adler, Sandhini Agarwal, Lama Ahmad, Ilge Akkaya, Florencia Leoni Aleman, Diogo Almeida, Janko Altenschmidt, Sam Altman, Shyamal Anadkat, et al. 2023. Gpt-4 technical report. *arXiv preprint arXiv:2303.08774*.

Jean-Baptiste Alayrac, Jeff Donahue, Pauline Luc,

Antoine Miech, Iain Barr, Yana Hasson, Karel Lenc, Arthur Mensch, Katherine Millican, Malcolm Reynolds, et al. 2022. Flamingo: a visual language model for few-shot learning. *Advances in Neural Information Processing Systems*.

Liang Chen, Haozhe Zhao, Tianyu Liu, Shuai Bai, Junyang Lin, Chang Zhou, and Baobao Chang. 2024. An image is worth 1/2 tokens after layer 2: Plug-and-play inference acceleration for large vision-language models. In *Proceedings of the European Conference on Computer Vision*.

Zesen Cheng, Sicong Leng, Hang Zhang, Yifei Xin, Xin Li, Guanzheng Chen, Yongxin Zhu, Wenqi Zhang, Ziyang Luo, Deli Zhao, et al. 2024. Videollama 2: Advancing spatial-temporal modeling and audio understanding in video-llms. *arXiv preprint arXiv:2406.07476*.

Wei-Lin Chiang, Zhuohan Li, Zi Lin, Ying Sheng, Zhanghao Wu, Hao Zhang, Lianmin Zheng, Siyuan Zhuang, Yonghao Zhuang, Joseph E Gonzalez, et al. 2023. Vicuna: An open-source chatbot impressing gpt-4 with 90%\* chatgpt quality. URL <https://vicuna.lmsys.org>.

Xiangxiang Chu, Limeng Qiao, Xinyang Lin, Shuang Xu, Yang Yang, Yiming Hu, Fei Wei, Xinyu Zhang, Bo Zhang, Xiaolin Wei, et al. 2023. Mobilevlm: A fast, reproducible and strong vision language assistant for mobile devices. *arXiv preprint arXiv:2312.16886*.

Wenliang Dai, Junnan Li, Dongxu Li, Anthony Meng Huat Tiong, Junqi Zhao, Weisheng Wang, Boyang Li, Pascale Fung, and Steven Hoi. 2023. Instructblip: Towards general-purpose vision-language models with instruction tuning. *arXiv preprint arXiv:2305.06500*.

Kai Han, Jianyuan Guo, Yehui Tang, Wei He, Enhua Wu, and Yunhe Wang. 2024. Free video-llm: Prompt-guided visual perception for efficient training-free video llms. *arXiv preprint arXiv:2410.10441*.

Peng Jin, Ryuichi Takanobu, Wancai Zhang, Xiaochun Cao, and Li Yuan. 2024. Chat-univi: Unified visual representation empowers large language models with image and video understanding. In *Proceedings of the IEEE Conference on Computer Vision and Pattern Recognition*.

Wonkyun Kim, Changin Choi, Wonseok Lee, and Wonjong Rhee. 2024. An image grid can be worth a video: Zero-shot video question answering using a vlm. *arXiv preprint arXiv:2403.18406*.

Bo Li, Yuanhan Zhang, Dong Guo, Renrui Zhang, Feng Li, Hao Zhang, Kaichen Zhang, Yanwei Li, Ziwei Liu, and Chunyuan Li. 2024. Llava-onevision: Easy visual task transfer. *arXiv preprint arXiv:2408.03326*.

- Junnan Li, Dongxu Li, Silvio Savarese, and Steven Hoi. 2023a. Blip-2: Bootstrapping language-image pre-training with frozen image encoders and large language models. In *Proceedings of the International Conference on Machine Learning*.
- KunChang Li, Yinan He, Yi Wang, Yizhuo Li, Wenhai Wang, Ping Luo, Yali Wang, Limin Wang, and Yu Qiao. 2023b. Videochat: Chat-centric video understanding. *arXiv preprint arXiv:2305.06355*.
- Yuncheng Li, Yale Song, Liangliang Cao, Joel Tetreault, Larry Goldberg, Alejandro Jaimes, and Jiebo Luo. 2016. Tgif: A new dataset and benchmark on animated gif description. In *Proceedings of the IEEE Conference on Computer Vision and Pattern Recognition*.
- Bin Lin, Yang Ye, Bin Zhu, Jiayi Cui, Munan Ning, Peng Jin, and Li Yuan. 2023. Video-llava: Learning united visual representation by alignment before projection. *arXiv preprint arXiv:2311.10122*.
- Haotian Liu, Chunyuan Li, Yuheng Li, and Yong Jae Lee. 2024a. Improved baselines with visual instruction tuning. In *Proceedings of the IEEE Conference on Computer Vision and Pattern Recognition*.
- Haotian Liu, Chunyuan Li, Yuheng Li, Bo Li, Yuanhan Zhang, Sheng Shen, and Yong Jae Lee. 2024b. Llava-next: Improved reasoning, ocr, and world knowledge. URL <https://llava-vl.github.io/blog/2024-01-30-llava-next/>.
- Haotian Liu, Chunyuan Li, Qingyang Wu, and Yong Jae Lee. 2024c. Visual instruction tuning. *Advances in Neural Information Processing Systems*, 36.
- Fan Ma, Xiaojie Jin, Heng Wang, Yuchen Xian, Jiashi Feng, and Yi Yang. 2023. Vista-llama: Reliable video narrator via equal distance to visual tokens. *arXiv preprint arXiv:2312.08870*.
- Muhammad Maaz, Hanoona Rasheed, Salman Khan, and Fahad Shahbaz Khan. 2024. Video-chatgpt: Towards detailed video understanding via large vision and language models. In *Association for Computational Linguistics*.
- Karttikeya Mangalam, Raiymbek Akshulakov, and Jitendra Malik. 2023. Egoschema: A diagnostic benchmark for very long-form video language understanding. *Advances in Neural Information Processing Systems*.
- Long Ouyang, Jeffrey Wu, Xu Jiang, Diogo Almeida, Carroll Wainwright, Pamela Mishkin, Chong Zhang, Sandhini Agarwal, Katarina Slama, Alex Ray, et al. 2022. Training language models to follow instructions with human feedback. *Advances in Neural Information Processing Systems*.
- Alec Radford, Jong Wook Kim, Chris Hallacy, Aditya Ramesh, Gabriel Goh, Sandhini Agarwal, Girish Sastry, Amanda Askell, Pamela Mishkin, Jack Clark, et al. 2021. Learning transferable visual models from natural language supervision. In *Proceedings of the International Conference on Machine Learning*.
- Yuzhang Shang, Mu Cai, Bingxin Xu, Yong Jae Lee, and Yan Yan. 2024. Llava-prumerge: Adaptive token reduction for efficient large multimodal models. *arXiv preprint arXiv:2403.15388*.
- Enxin Song, Wenhao Chai, Guan hong Wang, Yucheng Zhang, Haoyang Zhou, Feiyang Wu, Haozhe Chi, Xun Guo, Tian Ye, Yanting Zhang, et al. 2024a. Moviechat: From dense token to sparse memory for long video understanding. In *Proceedings of the IEEE Conference on Computer Vision and Pattern Recognition*.
- Enxin Song, Wenhao Chai, Tian Ye, Jenq-Neng Hwang, Xi Li, and Gaoang Wang. 2024b. Moviechat+: Question-aware sparse memory for long video question answering. *arXiv preprint arXiv:2404.17176*.
- Rohan Taori, Ishaan Gulrajani, Tianyi Zhang, Yann Dubois, Xuechen Li, Carlos Guestrin, Percy Liang, and Tatsunori B Hashimoto. 2023. Stanford alpaca: An instruction-following llama model.
- Gemini Team, Rohan Anil, Sebastian Borgeaud, Jean-Baptiste Alayrac, Jiahui Yu, Radu Soricut, Johan Schalkwyk, Andrew M Dai, Anja Hauth, Katie Millican, et al. 2023. Gemini: a family of highly capable multimodal models. *arXiv preprint arXiv:2312.11805*.
- Hugo Touvron, Thibaut Lavril, Gautier Izacard, Xavier Martinet, Marie-Anne Lachaux, Timothée Lacroix, Baptiste Rozière, Naman Goyal, Eric Hambro, Faisal Azhar, et al. 2023a. Llama: Open and efficient foundation language models. *arXiv preprint arXiv:2302.13971*.
- Hugo Touvron, Louis Martin, Kevin Stone, Peter Albert, Amjad Almahairi, Yasmine Babaei, Nikolay Bashlykov, Soumya Batra, Prajjwal Bhargava, Shruti Bhosale, et al. 2023b. Llama 2: Open foundation and fine-tuned chat models. *arXiv preprint arXiv:2307.09288*.
- Zhongwei Wan, Ziang Wu, Che Liu, Jinfa Huang, Zhihong Zhu, Peng Jin, Longyue Wang, and Li Yuan. 2024. Look-m: Look-once optimization in kv cache for efficient multimodal long-context inference. *arXiv preprint arXiv:2406.18139*.
- Lean Wang, Lei Li, Damai Dai, Deli Chen, Hao Zhou, Fandong Meng, Jie Zhou, and Xu Sun. 2023. Label words are anchors: An information flow perspective for understanding in-context learning. In *Proceedings of the Conference on Empirical Methods in Natural Language Processing*.
- Xiaohan Wang, Yuhui Zhang, Orr Zohar, and Serena Yeung-Levy. 2024a. Videoagent: Long-form video understanding with large language model as agent. *arXiv preprint arXiv:2403.10517*.

- Ziyang Wang, Shoubin Yu, Elias Stengel-Eskin, Jaehong Yoon, Feng Cheng, Gedas Bertasius, and Mohit Bansal. 2024b. Videotree: Adaptive tree-based video representation for llm reasoning on long videos. *arXiv preprint arXiv:2405.19209*.
- Wenhao Wu. 2024. Freeva: Offline mllm as training-free video assistant. *arXiv preprint arXiv:2405.07798*.
- Junbin Xiao, Xindi Shang, Angela Yao, and Tat-Seng Chua. 2021. Next-qa: Next phase of question-answering to explaining temporal actions. In *Proceedings of the IEEE Conference on Computer Vision and Pattern Recognition*.
- Lin Xu, Yilin Zhao, Daquan Zhou, Zhijie Lin, See Kiong Ng, and Jiashi Feng. 2024a. Pllava: Parameter-free llava extension from images to videos for video dense captioning. *arXiv preprint arXiv:2404.16994*.
- Mingze Xu, Mingfei Gao, Zhe Gan, Hong-You Chen, Zhengfeng Lai, Haiming Gang, Kai Kang, and Afshin Dehghan. 2024b. Slowfast-llava: A strong training-free baseline for video large language models. *arXiv preprint arXiv:2407.15841*.
- Zhou Yu, Dejing Xu, Jun Yu, Ting Yu, Zhou Zhao, Yueting Zhuang, and Dacheng Tao. 2019. Activitynet-qa: A dataset for understanding complex web videos via question answering. In *Proceedings of the AAAI Conference on Artificial Intelligence*.
- Ce Zhang, Taixi Lu, Md Mohaiminul Islam, Ziyang Wang, Shoubin Yu, Mohit Bansal, and Gedas Bertasius. 2023a. A simple llm framework for long-range video question-answering. *arXiv preprint arXiv:2312.17235*.
- Hang Zhang, Xin Li, and Lidong Bing. 2023b. Video-llama: An instruction-tuned audio-visual language model for video understanding. *arXiv preprint arXiv:2306.02858*.
- Yuanhan Zhang, Bo Li, haotian Liu, Yong jae Lee, Liangke Gui, Di Fu, Jiashi Feng, Ziwei Liu, and Chunyuan Li. 2024. Llava-next: A strong zero-shot video understanding model. URL <https://llava-vl.github.io/blog/2024-04-30-llava-next-video/>.

Method	LLM Size	Vision Encoder	Open-Ended VideoQA		Multiple Choice VideoQA		VCGBench Avg Score
			ANet-QA Accuracy/Score	TGIF-QA Accuracy/Score	NExTQA Accuracy	EgoSchema Accuracy	
Video-LLaMA2 (Cheng et al., 2024)	46.7B	CLIP-L	50.3/3.4	-	-	53.3	3.15
PLLaVA (Xu et al., 2024a)	34B	CLIP-L	50.9/3.7	80.6/4.3	-	-	-
LLaVA-NeXT-Video (Zhang et al., 2024)	34B	CLIP-L	58.8/3.4	-	-	-	3.34
LLaVA-NeXT-Video-DPO (Zhang et al., 2024)	34B	CLIP-L	64.4/3.6	-	-	-	3.77
IG-VLM (Kim et al., 2024)	34B	CLIP-L	58.4/ <b>3.5</b>	79.1/4.2	70.9	53.6	3.09
SF-LLaVA (Xu et al., 2024b)	34B	CLIP-L	59.2/ <b>3.5</b>	80.6/ <b>4.3</b>	72.0	55.8	3.32
<b>LLaVA-MLB<sup>G</sup></b>	34B	CLIP-L	<b>59.4/3.5</b>	<b>81.9/4.2</b>	73.5	<b>57.4</b>	3.34
<b>LLaVA-MLB<sup>G+S</sup></b>	34B	CLIP-L	58.9/ <b>3.5</b>	81.3/4.2	<b>73.6</b>	56.8	<b>3.35</b>

Table 8: Results of open-ended VideoQA, multiple choice VideoQA, and text generation using 34B LLMs.

VSTail Position	VCGBench (Score)					
	CI	DO	CU	TU	CO	Avg
None	3.18	<b>2.85</b>	3.55	2.45	3.29	3.06
Head	<b>3.22</b>	2.83	3.55	2.41	3.32	3.07
Tail*	<b>3.22</b>	2.83	<b>3.61</b>	<b>2.52</b>	<b>3.38</b>	<b>3.11</b>

Table 9: Ablation study on the VSTail’s summary sequence position in LLaVA-MLB<sup>G+S</sup>. None denotes no VSTail inclusion. Head and Tail refer to placing the summary sequence at the start and end of the visual input, respectively.

## Appendix

### A Experimental Settings

**Text Generation.** We evaluate video-to-text generation performance on VCGBench (Maaz et al., 2024), a benchmark comprising 500 videos sampled from ActivityNet-1.3 (Yu et al., 2019). Consistent with previous training-free methods (Kim et al., 2024; Xu et al., 2024b), we use the GPT-3.5-Turbo-0125 model to assign relative scores to model outputs across five dimensions: **C**orrectness of **I**nformation (CI), **D**etail **O**rientation (DO), **C**ontextual **U**nderstanding (CU), **T**emporal **U**nderstanding (TU), and **C**onsistency (CO). The average score across these metrics (Avg Score) provides an overall performance assessment.

**Open-ended VideoQA.** The open-ended VideoQA task includes ActivityNet-QA (ANet-QA) (Yu et al., 2019) and TGIF-QA (Li et al., 2016), where Video LLMs generate open-ended answers based on both the video content and the query. These questions typically have single-word ground-truth answers. Following previous methods (Kim et al., 2024; Wu, 2024; Han et al., 2024; Xu et al., 2024b), we employ the GPT-3.5-Turbo-0125 model to evaluate the responses in terms of accuracy (true or false) and quality (scored from 0 to 5).

**Multiple Choice VideoQA.** Video LLMs are evaluated on their ability to select the correct answer

from a set of predefined options. We evaluate performance using the NExTQA (Xiao et al., 2021) and EgoSchema (Mangalam et al., 2023) benchmarks.

**Implementation Details** Following recent training-free methods (Kim et al., 2024; Han et al., 2024; Xu et al., 2024b), we employ the Image LLM, LLaVA-NeXT (Liu et al., 2024b), for video understanding without additional training. Each sampled frame from the input video is resized to  $336 \times 336$  and processed by the CLIP-L vision encoder (Radford et al., 2021), producing  $H \times W = 24 \times 24$  tokens. For a video, we sample  $(G_h G_w) \times F = 4 \times 5$  frames. In GAPool, attention scores are derived from the  $(k = 3)^{\text{th}}$  layer and the grid size is  $G_h \times G_w = 2 \times 2$ . The VSTail’s pooling size is  $S_h \times S_w = 3 \times 4$ . For further explanation, please see Section 3.5. The two-stage SegAttn with GAPool is labeled LLaVA-MLB<sup>G</sup>, while LLaVA-MLB<sup>G+S</sup> includes both GAPool and VSTail. When evaluating pre-filling times, Parallel denotes stage one executed in parallel across 4 A100 GPUs, while Sequential denotes it executed sequentially on a single A100 GPU.

### B More Results

#### B.1 Results with 34B LLMs

Table 8 shows the results with 34B LLMs, where our model outperforms prior approaches on all benchmarks. Specifically, our model improves accuracy by **1.3%** on TGIF-QA, **1.6%** on NExTQA, and **1.6%** on EgoSchema. These consistent improvements across 7B and 34B LLMs confirm our model’s robustness and generalizability.

#### B.2 Effect of Summary Sequence Position.

Further validation of the VSTail’s summary sequence position in LLaVA-MLB<sup>G+S</sup> is provided in Table 9. Head and None perform similarly across all metrics, suggesting that summary tokens at the beginning do not improve video comprehension

in Image LLMs. Conversely, when the summary sequence is placed at the end, Tail demonstrates marked improvements in CU, TU, and CO. While CI and DO (Correctness of Information and Detail Orientation) focus on evaluating detailed video comprehension, CU, TU, and CO (Contextual Understanding, Temporal Understanding, and Consistency) assess overall understanding. Compared to None, Tail (VSTail) enhances global knowledge of video content while retaining fine-grained comprehension.